Gene Expression, Vol. 11, pp. 1–12
Printed in the USA.

1052-2166/03 $20.00 + .00

www.cognizantcommunication.com

Embryonic Activation and Developmental Expression of the Murine Prion Protein Gene

G. MIELE,* A. R. ALEJO BLANCO,* H. BAYBUTT,† S. HORVAT,‡ J. MANSON,† AND M. CLINTON*[1]

*Department of Gene Expression & Development, Roslin Institute, Roslin, Midlothian, Scotland, EH25 9PS, UK
†BBSRC Institute for Animal Health Neuropathogenesis Unit, Ogston Building, West Mains Road, Edinburgh, Scotland, EH9 3JF, UK
‡Biotechnical Faculty, Zootechnical Department, University of Ljubljana, Slovenia

While it is well established that cellular prion protein (PrP^C) expression is required for the development of transmissible spongiform encephalopathies (TSEs), the physiological function of PrP^C has yet to be determined. A number of studies have examined PrP expression in different tissues and in the later stages of embryonic development. However, the relative levels of expression of PrP RNA and protein in tissues outside the central nervous system (CNS) is not well documented and the exact point of transcriptional activation of PrP during embryogenesis is unknown. We have studied PrP mRNA expression in murine embryos and both mRNA and protein expression in a variety of adult tissues. PrP RNA was detected at different levels in all tissues tested while PrP^C protein was detectable in all adult tissues tested with the exception of kidney and liver. RNA and protein levels were also assessed at four points during postnatal brain development and levels of both were seen to increase with development. We also established that, during embryogenesis, induction of PrP RNA expression occurs between E8.5 and E9, during the period of transition from anaerobic to aerobic metabolism. Preliminary experiments investigating the effects of superoxide radicals on PrP expression in cultured neuroblastoma and astrocyte cells support the suggestion that PrP^C forms part of a cellular antioxidant defense mechanism.

Prion protein expression Oxidative stress Superoxide radicals Whole-mount in situ hybridization Prion protein function

THE cellular prion protein (PrP^C) is a glycosylphosphatidylinositol (GPI) anchored protein of unknown function (44,45). It is well established that expression of this single-copy gene (*Prnp*) is required for the development of a group of fatal neurodegenerative disorders, known as transmissible spongiform encephalopathies (TSEs). These diseases manifest in a broad range of species and include BSE in cattle, scrapie in sheep, and Kuru, CJD, variant CJD, and GSS in humans. They are without precedence in that they may present as a result of genetic, sporadic, or infectious mechanisms (37). PrP^{Sc}, a protein that accumulates during disease pathogenesis, represents the only TSE-specific macromolecule identified to date (26,36). PrP^{Sc} is a partially protease-resistant isoform of PrP^C (26,36), a cellular protein derived from a single-copy, host-encoded gene (1,33). Both forms of PrP undergo identical patterns of posttranslational modification (14) and apparently differ only with respect to α-helical and β-sheet content (34). To gain insight into the physiological function of PrP^C, mice that do not express PrP^C ($Prnp^{-/-}$ mice) have been generated and analyzed. These mice apparently develop and reproduce normally (8,23), although $Prnp^{-/-}$ mice are resistant to experimental TSE infection (12,24,41). Various phenotypes associated with $Prnp^{-/-}$ mice have been reported that may provide clues to the physiological function of PrP. These include a marked reduction in hippocampal and myocardial mitochondrial numbers (28), abnormal hippocampal synaptic plas-

Accepted October 16, 2002.
[1]Address correspondence to M. Clinton, Department of Gene Expression & Development, Roslin Institute, Roslin, Midlothian, Scotland, EH25 9PS, UK. Tel: +44 131 527 4216; Fax: +44 131 440 0434; E-mail: michael.clinton@bbsrc.ac.uk

ticity, weakened γ-aminobutyric acid type A receptor-mediated fast inhibition (11), and altered circadian rhythms and sleep patterns (51). In biochemical studies, PrP^C has been shown to bind copper directly (2,47) and to affect the activity of the antioxidant enzyme copper/zinc-dependent superoxide dismutase (Cu/Zn SOD) (4). *Prnp*$^{-/-}$ cells have also been shown to be more susceptible to treatment with superoxide radicals (4), and recent studies have indicated that PrP^C may possess antioxidant enzyme activity (5). These studies may implicate PrP^C as a participant in the cellular response to oxidative stress.

PrP mRNA and protein expression have also been studied on the basis that location and level of expression may provide clues to function. The steady-state levels of PrP mRNA have been assessed in a number of studies and it is obvious that PrP RNA expression is widespread in adult rodent tissues, with highest levels reported for the brain and lowest levels for spleen and liver (9,33,38). PrP RNA has also been shown to be expressed during the later stages of embryogenesis and to be developmentally regulated in a variety of species (13,16,20,21,25,27,31,48). Despite these studies, the relative levels of PrP mRNA in various adult non-CNS tissues has not been documented in detail and the precise stage of transcriptional activation of PrP during embryogenesis has yet to be established. Establishing the timing and distribution of PrP expression during embryogenesis and the relative levels of mRNA and protein in a variety of tissues may aid in our understanding of both PrP^C function and of the process of neuroinvasion and pathogenesis following exposure to the TSE agent.

Here we have analyzed the expression of the PrP transcript and protein in a variety of murine adult tissues and in the postnatal developing brain. We have also characterized the expression of the PrP transcript at various stages of murine embryogenesis to establish the point of transcriptional activation. In light of these and other recently published results, we have investigated the effects of exposure to oxidative stress mediated by superoxide radicals on PrP RNA expression in cultured neuronal and glial cells.

MATERIALS AND METHODS

Animals

To provide tissues for RNA extraction, postnatal (P) mice (129/Ola strain) were sacrificed on the day of birth (P1), and 10, 20, and 42 days after birth (P10, P20, P42). Mice homozygous for a null mutation in the *Prnp* gene (*Prnp*$^{-/-}$) have been described elsewhere (23). For protein analyses, tissues were collected from 129/Ola mice, with the exception of those used for postnatal developing brain PrP^C, which were of the C57BL strain. Various tissues were collected, flash-frozen in liquid nitrogen, and stored at −80°C until required. Murine embryos collected for RT-PCR and whole-mount in situ hybridization experiments were of the C57BL/6J strain. Embryos were staged according to standard descriptions (18).

Isolation of Total RNA

Individual tissues and embryos (collected at 9, 11, 13, 15, and 17 days postcoitum, dissected free of extra embryonic tissues, and stored at −80°C) were pooled and total RNA isolated using a variable speed polytron homogenizer and RNAzol™ B (AMS Biotechnology, Oxon, UK) according to the manufacturer's instructions. Total RNA was stored as an ethanolic precipitate at −20°C until required.

RT-PCR

First-strand cDNA was prepared using a cDNA Synthesis Kit and a *Not*I-d$(T)_{18}$ primer according to the manufacturer's instructions (Amersham Pharmacia Biotech, Bucks, UK) and 5 μg of total RNA (prepared from embryos pooled from several pregnancies) pretreated with DNase (RQ1 RNase-free DNase; Promega, Southampton, UK). First-strand cDNA reactions were performed with (RT+) or without (RT−) reverse transcriptase in a 15 μl volume. cDNA equivalent to 33 ng of total RNA was used as template. Primers specific for PrP exon 3 (forward, 5′-GATC CATTTTGGCAACGACT-3′; reverse, 5′-ATCCCAC GATCAGGAAGATG-3′) were used for PCR reactions that generated a 371-bp product. PCR reactions (40 μl) contained 10 mM Tris-HCl, 1.5 mM $MgCl_2$, 50 mM KCl (pH 8.3), 1.25 μM of each primer, 200 μM dNTP, and 2.5 units of Taq polymerase (Boehringer Mannheim, East Sussex, UK). PCR cycling conditions were 1 cycle of 94°C for 2 min, 35 cycles of 94°C for 30 s (30 cycles for β-actin RT-PCR), 65°C for 30 s, 72°C for 30 s followed by a final extension step of 72°C for 5 min. Primers and reaction conditions for RT-PCR of β-actin have been described previously (50). PrP and β-actin RT-PCR products (20 μl of PCR reaction) were analyzed in a 1% 1× TBE agarose gel. On completion of electrophoresis, the PrP RT-PCR products were transferred to Hybond®-N nylon membrane (Amersham Pharmacia Biotech) by standard capillary Southern blotting procedures (42).

Whole-Mount In Situ Hybridization (WM-ISH)

Embryos were collected at 8.5 and 9.5 days postcoitum. Following dissection in Ca^{2+}/Mg^{2+}-free PBS

(ICN Biomedicals Inc., OH) to remove extra embryonic membranes, the neural tube and heart were pierced with a needle to prevent trapping of reagents. The embryos were immediately prepared for WM-ISH by fixing in 4% paraformaldehyde/2 mM EGTA (BDH, Dorset, UK) overnight at 4°C.

The WM-ISH procedure was performed as previously described (53). pBluescript® KS II$^+$ vector (Stratagene, The Netherlands) containing a 930-bp *Kpn*I-*Eco*RI fragment of *Prnp* exon 3 was used as template to synthesize digoxygenin (DIG)-labeled sense and antisense riboprobes using a DIG-labeling RNA synthesis kit and T7/T3 RNA polymerases (Roche Diagnostics, East Sussex, UK) according to the manufacturer's instructions. Prior to hybridization, riboprobes were hydrolyzed to a size of approximately 200 nt as previously described (53).

Proteinase K (Life Technologies, Paisley, UK) treatment of embryos was performed at a concentration of 10 μg/ml for 10 min and 15 min for E8.5 and E9.5 embryos, respectively.

Following hybridization (performed at 63°C overnight) and washing, bound DIG-labeled riboprobe was detected using an anti-DIG alkaline phosphatase-conjugated antibody (Boehringer Mannheim) at a dilution of 1:2500. Color development was performed for 3 or 6 h (E9.5 and E8.5 embryos, respectively) and embryos were subsequently postfixed in 4% paraformaldehyde and stored at 4°C.

For photography, embryos were positioned on 0.8% agarose solid support and photographed using dark-field microscopy.

Northern Blot Analysis

RNA was resuspended in buffer containing 10% v/v MOPS, 6.5% v/v formaldehyde, and 50% formamide and incubated at 65°C for 10 min. Heat-denatured total RNA (20 μg) was loaded onto a 1% agarose gel (containing 7% v/v formaldehyde) and electrophoresis was performed at 80 V for 3 h. RNA was transferred in 10× SSC, to a Hybond®-N membrane (Amersham Pharmacia Biotech) by capillary action. Membranes were rinsed briefly in 2× SSC and baked at 80°C for 2 h. Membranes were prehybridized in 20 ml of 0.5 M Na_2HPO_4/7% SDS, containing 100 μg/ml of denatured salmon sperm DNA (Life Technologies, Paisley, UK) and 20 μg/ml tRNA (Sigma Chemical Co., Dorset, UK) for 1 h at 65°C. Membranes were hybridized with a 930-bp PrP fragment (exon 3, *Kpn*I-*Eco*RI) labeled with [α-^{32}P]dCTP (3000 Ci/mmol) using a Rediprime II labeling system according to the manufacturer's instructions. Denatured radiolabeled probe was added to the hybridization solution at a concentration of 1×10^6 cpm/ml and hybridized overnight at 65°C. Membranes were washed once for 15 min at room temperature and once for 20 min at 65°C in 25 mM Na_2HPO_4/1% SDS and exposed to autoradiographic film. For Northern analyses, hybridization signal was quantitated using a PhosphorImager (Molecular Dynamics, Sunnyvale, CA). The membranes were stripped and subsequently rehybridized with a 255-bp 18S rRNA cDNA probe (29). Quantitation of 18S rRNA signal was used to adjust the PrP values to account for variations in RNA loading.

To establish the relative levels of expression in mouse tissues, a series of Northern hybridizations was prepared (using RNA isolated from pools of tissues from several animals) and probed with a radiolabeled PrP probe. Signals were quantitated, and membranes stripped and rehybridized with a probe to 18S rRNA to adjust PrP values for RNA loading variations. Three individual Northern analyses were performed for each tissue sample.

Western Analysis of Proteins

For Western analysis of PrP^C and actin proteins, tissues were processed essentially as previously described to obtain enriched membrane preparations from tissues (17). Briefly, tissues were homogenized in 10 mM Tris-HCl, pH 8, containing protease inhibitors (Roche Diagnostics). Samples were centrifuged for 20 min, the supernatant was removed, and the pellets resuspended in 10 mM Tris-HCl, pH 8, 150 mM NaCl, 1% Triton X-100, 0.5% deoxycholic acid, 0.1% SDS, and 5 mM EDTA. Following determination of protein concentration by Bradford assay, SDS-PAGE loading buffer, containing DTT, was added to the sample and 70 μg of protein extract denatured at 99°C for 5 min prior to loading onto Novex 12% Tris-glycine SDS polyacrylamide gels (Invitrogen Life Technologies, Paisley, UK). Electrophoresis was performed at 40 mA for approximately 2 h. Proteins were transferred to PVDF membranes at 150 mA for approximately 90 min. Western analysis was performed with a 1:2000 dilution of rabbit anti-mouse PrP^C [1B3 (12)] or a 1:500 dilution of goat anti-mouse PrP^C (M20, Autogen Bioclear, Wiltshire, UK) or a 1:500 dilution of goat anti-mouse β-actin (Autogen Bioclear), followed by horseradish peroxidase-linked donkey anti-goat IgG. Blots hybridized with anti-PrP^C were stripped prior to reprobing with anti-actin antibodies. Signal was visualized by ECL chemiluminescence (Amersham Pharmacia Biotech).

Treatment of Cultured Cells With Superoxide Radicals

Cultured cells were prepared from murine adult brain essentially as described previously (3). Glial

cells were derived from these primary cultures and utilized at passage 12. The glial cell cultures were determined by immunofluoresence to be composed predominantly of astrocytes, as indicated by the astrocyte cell marker glial fibrillary acidic protein (GFAP) (data not shown). Murine neuroblastoma (Neuro-2a) cells were obtained from the American Tissue Culture Center (Manassas, VA).

Cells were plated at equivalent densities in six-well culture dishes (Corning Costar, Bucks, UK) and maintained in Dulbecco's minimal essential medium (Life Technologies), supplemented with 10% fetal calf serum, at 37°C/5% CO_2. Cells were treated with 5 μM xanthine substrate, either alone or in combination with various concentrations of xanthine oxidase (Boehringer Mannheim) as a source of superoxide radicals. Xanthine oxidase treatment was carried out at approximately 60% confluency and the cells maintained for a further 24 h. Treatments were performed in triplicate. Cells were subsequently rinsed with PBS (Life Technologies), harvested, and total RNA isolated from combined triplicate experiments. Total RNA (20 μg N2a RNA, 15 μg astrocyte RNA) was used for Northern analysis to establish levels of PrP RNA in treated compared to untreated cells.

RESULTS

Embryonic Expression of PrP RNA

RT-PCR analysis was performed on RNA isolated from whole mouse embryos in order to determine the point in embryonic development at which activation of PrP gene expression occurs. Figure 1 shows PrP RT-PCR amplification of PrP in developing embryos (E9 to E17). The same cDNA samples were used for all RT-PCR reactions. PrP RT-PCR product was readily detected by ethidium bromide staining in embryos at all stages examined with the exception of E9. PCR products were of the expected size and were present only in RT+ reactions, demonstrating specificity for cDNA as opposed to contaminating genomic DNA (Fig. 1a). Following capillary transfer, Southern hybridization of PCR products with a radiolabeled PrP probe clearly confirmed that RT-PCR products were PrP specific, with noticeably lower levels at E9 (Fig. 1b). Amplification of β-actin by RT-PCR produces similar quantities of product for all embryonic stages, suggesting that the lower levels of PrP observed at E9 do not result from variation in cDNA synthesis (Fig. 1c). The hybridization of PCR products with a PrP-specific probe confirms both the specificity of the reactions and the lower levels of expression in E9 embryos. This experiment (Fig. 1b) demonstrates low-level PrP expression in E9 embryos, which could not be reliably demonstrated by ethidium bromide staining (Fig. 1a).

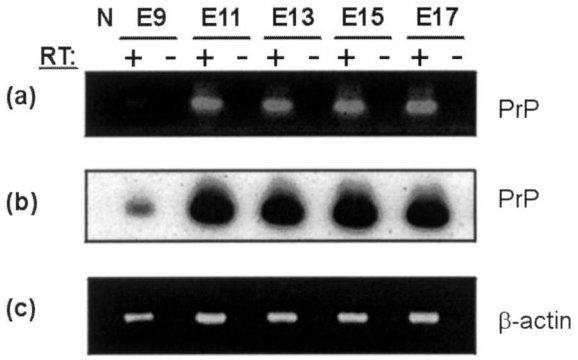

Figure 1. Measurement of PrP expression in the developing murine embryo by RT-PCR. First-strand cDNA synthesis was performed on 5 μg of DNase-treated total RNA extracted from murine embryos at E9, E11, E13, E15, and E17 stages of development [with (+) or without (–) RT]. A control in which template cDNA was omitted was also included (N). (a) Ethidium bromide-stained agarose gel following electrophoresis of RT-PCR products of exon 3 of the *Prnp* gene. (b) Southern analysis of gel depicted in (a), probed with a radiolabeled 930-bp *Kpn*I-*Eco*RI PrP DNA. (c) Ethidium bromide-stained agarose gel following electrophoresis of RT-PCR products of β-actin.

To establish both the exact timing of PrP transcriptional activation and the initial spatial expression pattern of PrP transcripts, we selected embryos at E8.5 and E9.5 stages of embryogenesis for further analysis by WM-ISH. PrP RNA expression was undetectable in the E8.5 embryo (Fig. 2b) by the WM-ISH procedures utilized here. No expression was detected in the primitive forebrain, midbrain, or hindbrain regions, and while there appeared to be very weak staining in the region posterior to the optic eminence, this most likely represents background staining because this signal was not detectable in other embryos of this stage. In contrast to the lack of expression in E8.5 embryos, PrP RNA expression was widespread throughout all regions of the developing brain by the E9.5 stage of embryogenesis (Fig. 2d–f). PrP staining could be detected in the telencephalic, mesencephalic, and metencephalic vesicles and appeared to be limited to the differentiating neuroepithelium of these structures. In addition, low-level expression of PrP was also detectable in the developing neural tube, again apparently associated with the differentiating neuroepithelium (Fig. 2e). Although there was no clear expression in the peripheral nervous system (PNS) at the E9.5 stage, a faint signal suggests that PrP RNA may be expressed at a low level at this stage in the otic pits (Fig. 2d, e) and possibly in the optic eminence (Fig. 2d), structures that develop into the auditory and optic systems, respectively. No signal was detected in embryos hybridized with the PrP sense probe (Fig. 2a, c).

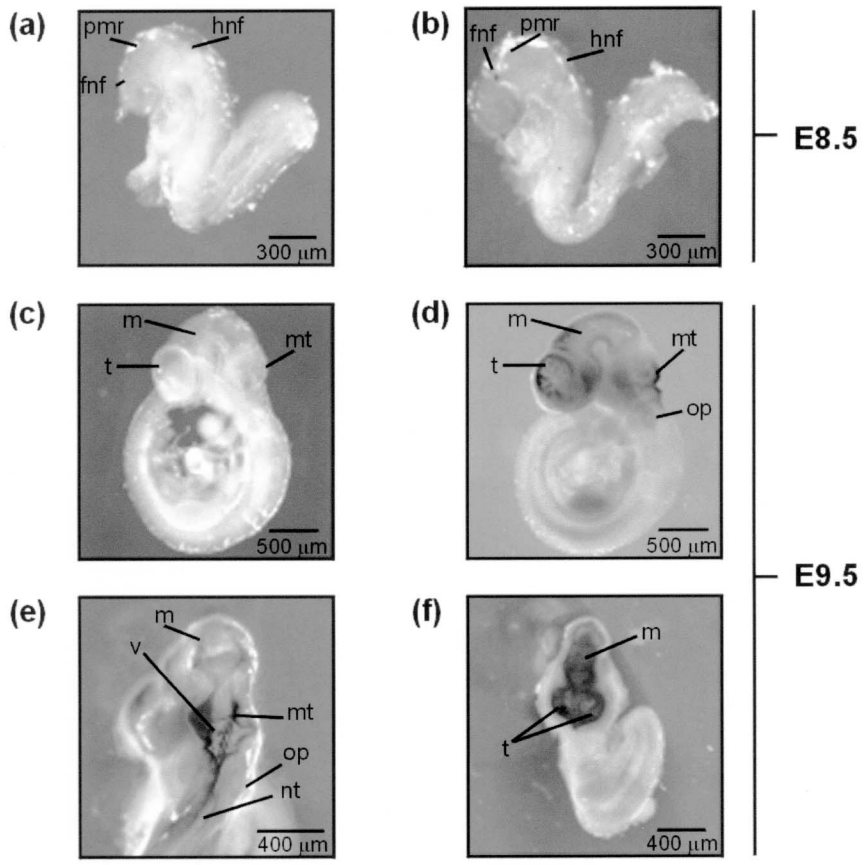

Figure 2. WM-ISH analysis of PrP expression in the developing murine embryo. E8.5 and E9.5 embryos hybridized with a DIG-labeled PrP sense (a, c) and antisense (b, d, e, f) riboprobe. Lateral (a, b, c, d), dorsal (e), and ventral (f) views. Probe hybridization was detected using an alkaline phosphatase-linked anti-DIG alkaline phosphatase-linked antibody. Color development was performed for 3 h (c, d, e, f) and 6 h (a, b). Abbreviations: pmr, prospective midbrain region; hnf, hindbrain neural fold; fnf, forebrain neural fold; t, telencephalon; m, mesencephalon; mt, metencephalon; op, otic pit; v, 4th ventricle (myelencephalon); nt, neural tube.

Postnatal and Adult Expression of PrP RNA

PrP RNA expression was studied in the murine postnatal developing brain and in other adult tissues by Northern analyses. In the developing brain, the primary 2.4-kb PrP transcript was readily detected, with highest levels in the P42 adult brain (Fig. 3a). PrP RNA levels increased in the developing brain approximately eightfold between the P1 and P42 period of postnatal development (Fig. 3a, c).

Transcripts of approximately 1.3 and 3.6 kb were also clearly detected in addition to the primary 2.4-kb PrP transcript in postnatal developing brain (Fig. 3a). As obvious from Figure 3a, the levels of these additional transcripts also increased during postnatal brain development. PhosphorImager analysis showed that they were present at levels equivalent to approximately 5% of the primary 2.4-kb transcript in adult brain. These PrP transcripts were not detectable in tissues in which the PrP gene had been ablated (Fig. 3b), suggesting that these transcripts are specific to the PrP locus. In addition, Southern blot analyses using this probe revealed only genomic DNA fragments of the predicted sizes (data not shown), indicating that the visualized transcripts do not result from hybridization to closely related genes.

Figure 3 also shows hybridization of PrP probe to RNA from various non-CNS murine tissues, demonstrating expression in all tissues examined (Fig. 3a, b). It is clear that in these tissues PrP RNA levels were highest in lung, kidney, and heart, lower in muscle and testis, and lowest in spleen and liver. Relative to adult brain (P42), in lung, kidney, and heart PrP RNA was expressed at levels of 8–10%, in muscle and testis at 5–6%, and in spleen and liver at 2–3% (Fig. 3c). In addition to the primary transcript of 2.4 kb, a secondary transcript of 1.3 kb was also present in heart and kidney. In contrast to adult brain, this transcript in heart was expressed at approximately 70% of the level of the primary 2.4-kb transcript.

Northern analysis demonstrated that expression of

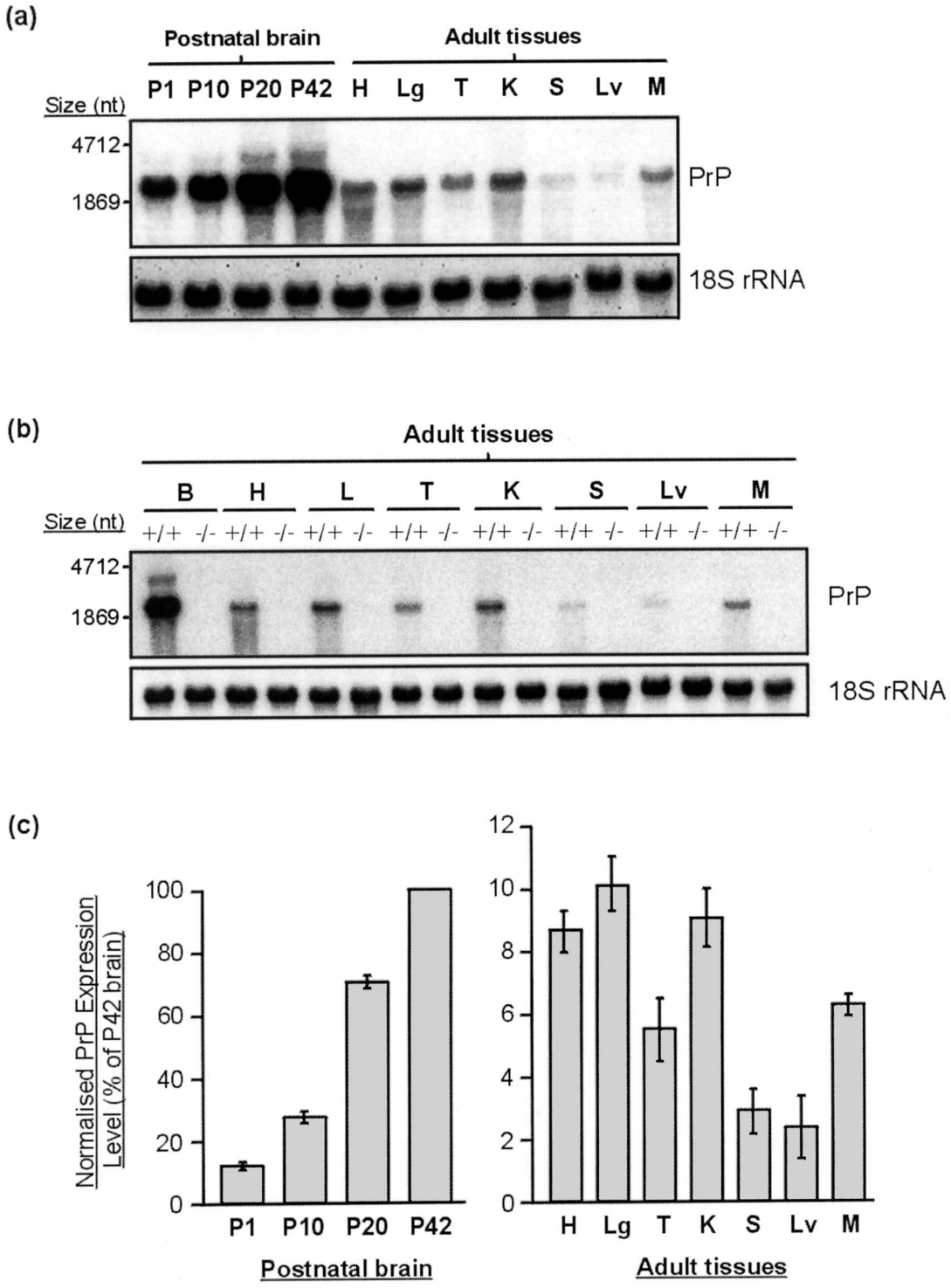

Figure 3. PrP RNA expression in postnatal and adult tissues. Total RNA was prepared from brains collected at 1 (P1), 10 (P10), 20 (P20), and 42 (P42) days of postnatal development (pooled from six animals), and from adult (P42) heart (H), lung (Lg), testis, (T), kidney (K), spleen (S), liver, (Lv), and skeletal muscle (M) (pooled from four animals). Denatured RNA (20 µg) was size fractionated through a 1% agarose gel, containing formaldehyde, transferred to Hybond®-N, and the membrane hybridized with a radiolabeled PrP probe (upper panel) and exposed to BiomaxMS autoradiography film (Sigma, Dorset, UK) for 24 h. Membranes were stripped and reprobed with an 18S rRNA cDNA probe (lower panel) to normalize for variations in RNA loading. The positions of 28S (4712 nt) and 18S (1869 nt) rRNA are indicated. (a) Expression of PrP in postnatal developing brain and various adult tissues. (b) Expression of PrP in various $Prnp^{+/+}$ and $Prnp^{-/-}$ tissues. (c) PrP phosphorimager values were adjusted in relation to 18S values and expressed as a percentage of PrP expression in the P42 adult brain. Shown are the means and SDs of values from three separate Northern blots. PrP RNA expression values are presented relative to values obtained for P42 brain.

PrP mRNA per microgram of total RNA was most abundant in adult brain and least abundant in spleen and liver (Fig. 3c). However, the yield of RNA per milligram wet weight of tissue varied greatly among different tissues. In absolute terms, when this variation is accounted for, PrP expression in the spleen represented 30% of PrP expression in the adult brain (data not shown).

Postnatal and Adult Levels of PrP^C Protein

Levels of PrP^C protein expression were studied in the murine postnatal developing brain and in adult tissues of *Prnp*$^{+/+}$ and *Prnp*$^{-/-}$ mice. In the developing brain, the primary 34-kDa PrP^C protein was readily detected, with highest levels in the P42 adult brain (Fig. 4a). The most significant increase in levels of PrP^C was observed from the P1 to P10 period of postnatal development.

Figure 4 also shows Western analysis of PrP^C from various non-CNS murine tissues. Protein extracts from *Prnp*$^{-/-}$ tissues analyzed in parallel in order to demonstrate which of the proteins reactive with the anti-mouse PrP^C antibody resulted from specific binding. While we examined the same representation of peripheral tissues as used for the RNA expression analysis outlined in Figure 3, PrP^C was only readily detectable in brain, heart, lung, testis, and skeletal muscle. Overexposure of blots revealed a faint PrP^C signal in spleen extracts using the M20 polyclonal antibody (data not shown). Based on equivalent protein loading, relative to adult (P42) brain, PrP^C levels were most abundant in heart and skeletal muscle, then testis and lung (Fig. 4b), then spleen (data not shown). We were unable to detect PrP^C in protein extracts from kidney or liver under the conditions outlined here, even following prolonged overexposures.

In addition to the primary 34-kDa PrP^C protein, Figures 4a and b shows the presence of lower molecular weight proteins that are reactive with the anti-

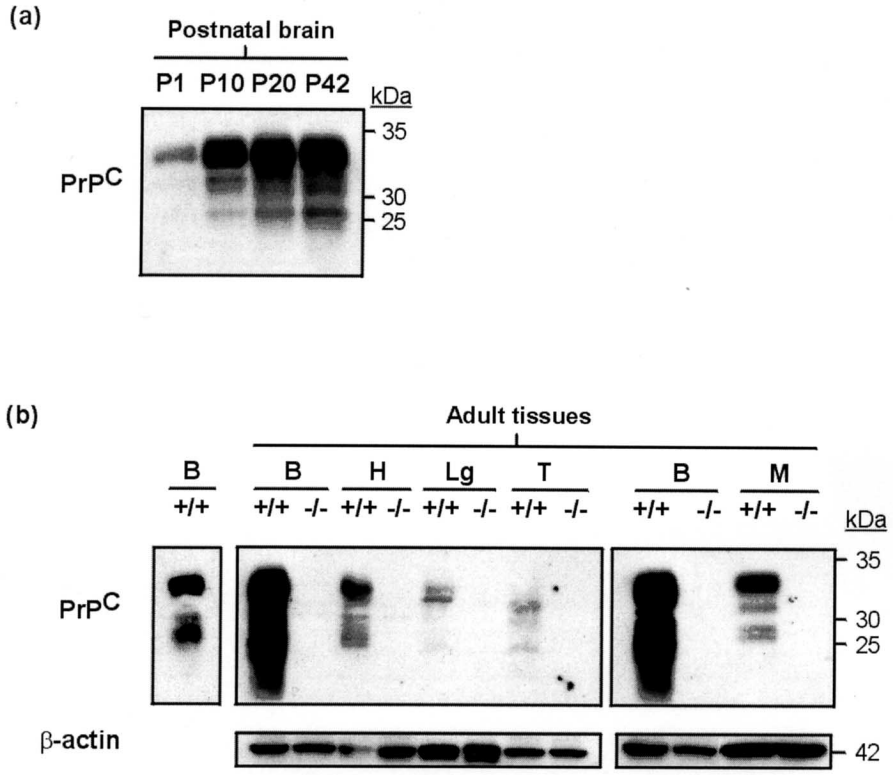

Figure 4. PrP^C expression in the postnatal developing brain and adult tissues. Protein extracts were prepared from brains collected at 1 (P1), 10 (P10), 20 (P20), and 42 (P42) days of postnatal development, and from adult (P42) heart (H), lung (Lg), testis, (T), spleen (S), and skeletal muscle (M) (pooled from two animals). Proteins (70 μg) were size fractionated through 16% SDS-PAGE gels, transferred to PVDF, and the membrane incubated with anti-mouse PrP^C (1B3, 1:2000) or anti-mouse β-actin antibodies (1:500), followed by HRP-linked anti-goat IgG. Actin was used to indicate approximately equivalent loading of proteins between *Prnp*$^{+/+}$ and *Prnp*$^{-/-}$ tissue pairs . Signals were detected by autoradiography following ECL chemiluminescence. The positions of molecular weight markers are indicated. (a) Expression of PrP^C in P1 to P42 developing brain. (b) PrP^C expression levels in adult (P42) tissues from *Prnp*$^{+/+}$ and *Prnp*$^{-/-}$ mice. The first lane represents a shorter exposure of the PrP^C signal in adult brain, to allow comparison of *Prnp*$^{+/+}$-specific PrP^C isoforms. Brain PrP^C signal is included in the following panels to indicate PrP^C levels in other tissues relative to P42 brain. Bands present in *Prnp*$^{+/+}$ tissues but not *Prnp*$^{-/-}$ tissues represent different isoforms of PrP^C.

mouse PrP^C antibody and that are specific to *Prnp*$^{+/+}$ tissues. In most tissues in which PrP^C was detectable, the major protein was approximately 34 kDa. However, in testis, the major PrP^C protein detected was approximately 31 kDa (Fig. 4b).

PrP RNA Levels Following Exposure to Superoxide Radicals

Murine neuroblastoma (N2a) cells and glial cells (predominantly astrocytes) derived from the primary culture of dissociated murine brain were used to investigate PrP RNA expression in response to exposure to superoxide radicals. Cultures were prepared in triplicate and pooled on completion of treatment. Cells were exposed for 24 h to varying degrees of oxidative stress induced by xanthine oxidase (a source of superoxide radicals), and then processed for RNA extraction. Northern blot analysis demonstrated that PrP RNA expression levels increased in response to exposure to superoxide radicals in both cell types in a dose-dependent fashion (Fig. 5a, b). PrP expression increased by up to 30% in N2a cells, while equivalent treatment (50 μU/ml of xanthine oxidase) induced an increase in PrP RNA expression of 60% in astrocytes (Fig. 5b).

DISCUSSION

At present, the precise molecular function of PrP^C is unclear. These studies were carried out on the basis that knowledge of the timing and distribution of PrP RNA and protein expression may aid our understanding of the function of PrP^C. Northern and Western analyses were used to characterize PrP RNA and protein expression in the postnatal developing brain and in various adult non-CNS tissues. To determine the point of transcriptional activation, we also analyzed PrP expression by both in situ hybridization and RT-PCR techniques at various stages of embryonic development between E8.5 and E17. We have established the relative levels of PrP RNA and protein in different murine adult tissues and demonstrated an eightfold increase in RNA levels in the brain between day 1 and day 42 of postnatal development. PrP^C protein levels also increase over this period, most significantly from P1 to P10. Although the increase in PrP RNA expression over this period has been previously reported, the eightfold increase reported here is greater than the fourfold increase in expression reported by others (20). It is also greater than that reported for postnatal developing rat (21) or hamster (27) brains. In addition to a primary PrP transcript of the expected size, we clearly demonstrate the existence of alternative forms of the PrP transcript in murine brain and in non-CNS tissues. While the smaller of these is similar to that previously reported by others in rodent tissues (33,38), the existence of a larger transcript is reported here for the first time. The significance of these additional transcripts and the possible relationship to alternative PrP transcripts reported in other species is unclear at present. Additionally, using protein extracts from enriched membrane preparations, we also clearly demonstrate the expression of PrP^C proteins that are smaller than the primary 34 kDa molecular weight of PrP^C and that are specific to *Prnp*$^{+/+}$ tissue protein extracts. In particular, in the testis the largest molecular weight PrP^C protein detected was approximately 31 kDa.

It has been documented previously that C-terminal truncated PrP^C isoforms are present in mature human sperm (43). Murine PrP^C is synthesized as a protein of 254 amino acids, which undergoes a variety of posttranslational modifications including removal of the N-terminal signal peptide, C-terminal cleavage, and glycosyl-phosphatidylinositol anchor addition (44). PrP^C also contains two *N*-glycosylation sequences, both of which can be variably glycosylated, giving rise to unglycosylated, monoglycosylated, and diglycosylated species (39,46). Therefore, because mature PrP^C is a heavily glycosylated protein that has undergone cleavage and removal of N- and C-terminal peptides, the different molecular weight isoforms detected in the tissues studied here most likely reflect different stages of protein biogenesis and/or differential complexities of glycosyl moieties. This suggestion is supported by the fact that following deglycosylation with PNGase, the major PrP-reactive band in all tissues studied was approximately 25–27 kDa (data not shown). With the exception of the kidney, the levels of PrP^C correlate well with the relative PrP RNA expression levels in murine tissues. While PrP RNA is apparently expressed at comparable levels in heart and kidney, of these tissues PrP^C protein could only be detected in protein extracts from heart under the experimental conditions outlined here. We were unable to detect PrP^C in enriched protein extracts from membranes from kidney using either the 1B3 rabbit anti-mouse polyclonal or the M20 goat anti-mouse PrP^C polyclonal (data not shown). This is in agreement with another report, which showed appreciable levels of PrP in RNA isolated from sheep kidney but failed to immunoprecipitate sheep PrP^C from kidney (32). It appears that while PrP RNA is readily detectable in kidney, in contrast to other peripheral tissues expressing PrP RNA, kidney does not represent a tissue in which PrP^C protein synthesis is detectable under these conditions. While it is possible that the kidney does not synthesize PrP protein, it is also possible that kidney PrP protein is not detectable by the

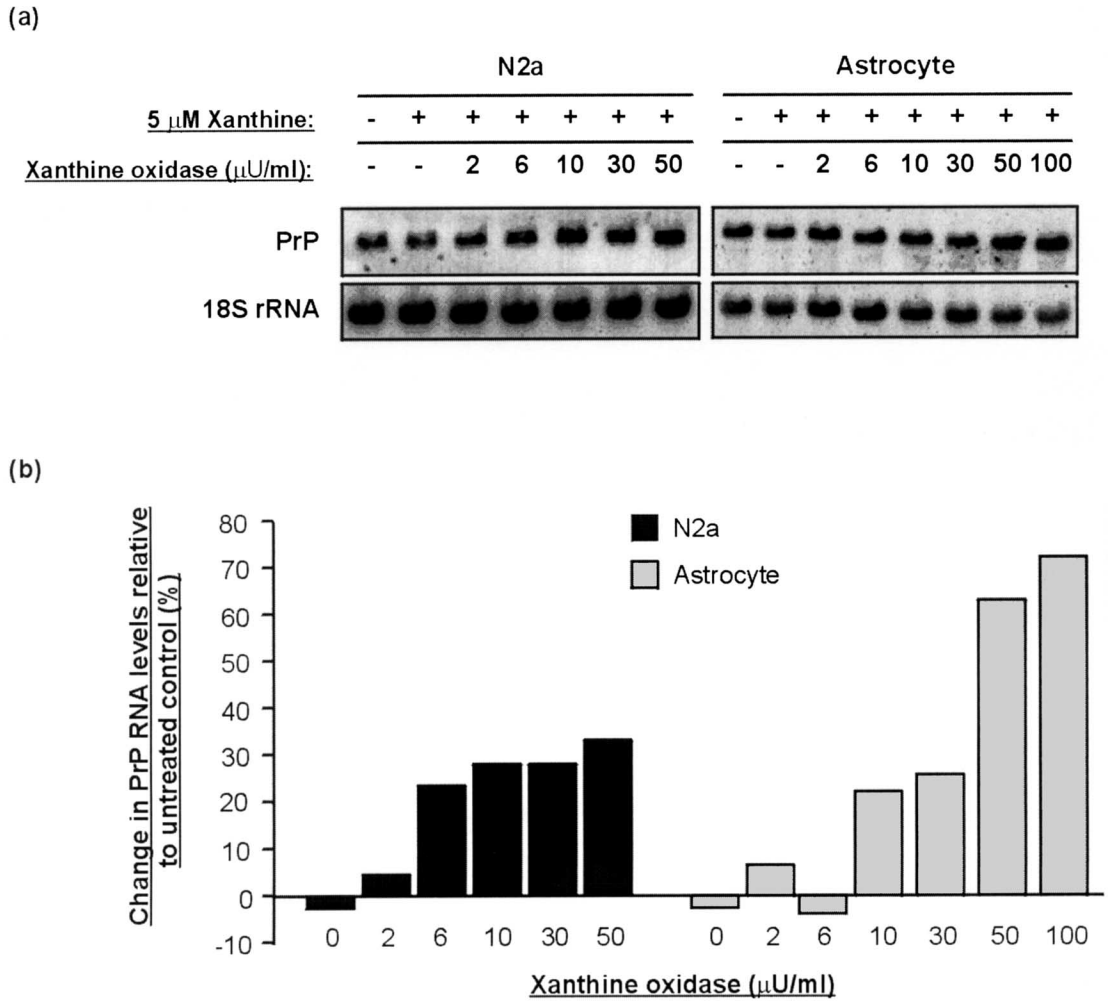

Figure 5. PrP RNA expression in murine neuroblastoma and astrocyte cells following exposure to superoxide radicals. (a) Northern analysis of PrP RNA and 18S rRNA in N2a and astrocyte cells treated with xanthine oxidase (source of superoxide radicals). (b) Quantitation of PrP RNA expression in treated cells. Quantitation of PrP RNA expression levels were adjusted for variations in RNA loading by 18S rRNA hybridization (lower panel) and quantitation. Values represent the percentage change in PrP RNA expression in cells exposed to superoxide radicals relative to untreated cells (corrected for loading variation by 18S rRNA hybridization and quantitation).

antibodies used under the conditions outlined in this study.

The levels of PrP RNA reported here for murine postnatal tissues have been calculated based on equivalent loading of RNA. It is of interest to note that when PrP RNA expression is calculated per unit weight of tissue (taking into consideration varying RNA contents of tissues), in absolute terms, the spleen is the highest non-CNS expressor of PrP RNA. This observation may prove to be of relevance in our understanding of the involvement of the lymphoreticular system in TSE disease pathogenesis, the spleen representing a major site of TSE agent replication prior to neuroinvasion (6,19).

While expression of PrP RNA throughout the CNS and PNS has previously been reported as early as E13.5 in the developing mouse embryo (25), by this stage of development expression is already widespread throughout the central and peripheral nervous system, and in nonneuronal structures. The precise stage of transcriptional activation of the PrP gene has not been previously described. The RT-PCR data presented in this article show that expression of PrP RNA is detectable by the E9 stage of embryogenesis. The lower level of PrP PCR product at E9 compared with all other stages suggests that E9 may be close to the point of transcriptional activation of PrP during murine embryogenesis. In accordance with this possibility, in situ hybridization experiments failed to detect PrP RNA expression in E8.5 embryos. In contrast, by the E9.5 stage of embryogenesis PrP RNA expression can be readily detected throughout the CNS; it appears to be limited to neural structures and is particularly evident in the differentiating neuroepithelium of

developing brain vesicles. As a consequence, we believe that PrP transcriptional activation occurs between E8.5 and E9 of murine embryogenesis (the neuralation stage). Our results represent the earliest demonstration of PrP RNA expression during embryogenesis and document the period of transcriptional activation of the PrP gene.

In developmental terms, the E8.5 to E9.5 period represents a dramatic stage of murine embryogenesis, as the processes of turning are initiated at this time and organogenesis is greatly accelerated (18,40). It has been recognized for some time that mammalian embryos are initially physiologically adapted for anaerobic (glycolytic) bioenergy production and later switch to aerobic (oxidative) metabolism (22,40). Murine embryos at E8.5 to E9.5 have approximately 8–20 somite pairs (18) and it is at this stage that the steady-state production of lactate drops and consequently the embryos' demand for oxygen grows (10, 15,30,49). Mitochondrial ultrastructure also becomes more characteristic of actively aerobically respiring cells as the embryo develops from the 8-somite stage (49). It is interesting to note that the PrP gene is transcriptionally activated during a period of embryogenesis when there is a shift in the type of bioenergy production utilized from anaerobic to aerobic metabolism. Aerobic metabolism carries with it the concomitant production of potentially damaging reactive oxygen species (ROS) intermediates, such as the superoxide radical. Presumably, antioxidant mechanisms to deal with generated ROS, such as the expression of superoxide dismutases, are also required during this stage of embryogenesis. It has been estimated that approximately 1–2% of the oxygen consumed for aerobic metabolism is converted to superoxide radicals, potentially capable of damaging DNA, lipid, and proteins (52,53). It could be speculated that using this form of bioenergy production requires the simultaneous onset of cellular antioxidant mechanisms with which to deal with ROS. Cu/Zn SOD is one such antioxidant enzyme and it has been demonstrated that activity of this copper-dependent enzyme is impaired in brains from mice devoid of PrP^C ($Prnp^{-/-}$) and that activity is elevated in brains of transgenic mice overexpressing PrP^C (4). This might result from PrP^C being a cuproprotein (2,47) and observations that Cu/Zn SOD receives copper from PrP^C (4). Therefore, a gene dosage effect of PrP on Cu/Zn SOD activity is clear. Additionally, recent studies suggest that PrP^C itself may possess SOD activity (5), and a potential role for PrP in the cellular response to oxidative stress seems likely from these studies. To explore this hypothesis, we performed preliminary experiments in which murine neural and astrocyte cells were exposed to varying doses of oxidative stress mediated by superoxide radicals and investigated the effect of this treatment on PrP RNA levels in these cells.

Expression of PrP RNA in cultured neuronal and astrocyte cells was shown to be regulated in a dose–response fashion in response to exposure to superoxide radicals. Exposure to increasing levels of superoxide radicals results in increased levels of PrP RNA in both cell types studied. From the data presented here, it seems likely that wild-type ($Prnp^{+/+}$) cells respond to increased ROS exposure by increased expression of PrP. Alternatively, as similar treatments with xanthine/xanthine oxidase have been shown to result in more pronounced cell death in $Prnp^{-/-}$ cells compared with $Prnp^{+/+}$ cells, it remains a possibility that superoxide treatment selects for those cells with higher levels of PrP expression. In any event, the preliminary data presented here further substantiate the notion that PrP^C forms part of a cellular antioxidant mechanism.

We suggest that PrP is activated during the embryonic E8.5 to E9 period as part of an antioxidant mechanism required to deal with elevated levels of ROS production, which occurs as aerobic metabolism begins. It is known that copper induces rapid endocytosis of PrP^C (35) and, therefore, the role of this protein in antioxidant defense might be via the provision of copper to the cytoslic Cu/Zn SOD. Alternatively, increased susceptibility of $Prnp^{-/-}$ cells and detection of increased levels of PrP RNA in response to exposure to superoxide radicals may indicate that PrP^C itself has more direct antioxidant capabilities. Indeed, recent evidence suggesting that both recombinant and immunoprecipitated PrP^C posses SOD activity supports this view (5).

In summary, we have documented the relative levels of PrP RNA and protein levels in postnatal developing brain and in various adult tissues. Additionally, we have shown that transcriptional activation of the PrP gene occurs during the E8.5 to E9 stage of murine embryogenesis. This represents the earliest demonstration of PrP expression during embryogenesis to date. Increased levels of PrP RNA in cultured cells exposed to superoxide radicals could suggest that initiation of PrP RNA expression during embryogenesis may be a response to ROS production by the onset of aerobic metabolism. Evidence accumulating to date strongly implicates PrP^C as having a physiological role in the cellular antioxidant response to oxidative stress.

ACKNOWLEDGMENTS

This work was supported by a BBSRC program grant (No. 210/BS204795) and by DEFRA (SE1759). 1B3 rabbit anti-mouse PrP^C polyclonal was a kind gift from C. Farquhar, Neuropathogenesis Unit, Edinburgh.

REFERENCES

1. Basler, K.; Oesch, B.; Scott, M.; Westaway, D.; Walchli, M.; Groth, D. F.; McKinley, M. P.; Prusiner, S. B.; Weissmann, C. Scrapie and cellular PrP isoforms are encoded by the same chromosomal gene. Cell 46:417–428; 1986.
2. Brown, D. R.; Qin, K.; Herms, J. W.; Madlung, A.; Manson, J.; Strome, R.; Fraser, P. E.; Kruck, T.; Von Bohlen, A.; Schulz-Schaeffer, W.; Giese, A.; Westaway, D.; Kretzschmar, H. The cellular prion protein binds copper in vivo. Nature 390:684–686; 1997.
3. Brown, D. R.; Schulz-Schaeffer, W. J.; Schmidt, B.; Kretzschmar, H. A. Prion protein-deficient cells show altered response to oxidative stress due to decreased SOD-1 activity. Exp. Neurol. 146:104–112; 1997.
4. Brown, D. R.; Besinger, A. Prion protein expression and superoxide dismutase activity. Biochem. J. 334: 423–429; 1998.
5. Brown, D. R.; Wong, B. S.; Hafiz, F.; Clive, C.; Haswell, S. J.; Jones, I. M. Normal prion protein has an activity like that of superoxide dismutatase. Biochem. J. 344:1–5; 1999.
6. Brown, K. L.; Stewart, K.; Ritchie, D. L.; Mabbott, N. A.; Williams, A.; Fraser, H.; Morrison, W. I.; Bruce, M. E. Scrapie replication in lymphoid tissues depends on prion protein expressing follicular dendritic cells. Nat. Med. 5:1308–1312; 1999.
7. Bueler, H.; Aguzzi, A.; Greiner, R. A.; Autenried, P.; Aguet, M.; Weissmann, C. Mice devoid of PrP are resistant to scrapie. Cell 73:1339–1347; 1993.
8. Bueler, H.; Fischer, M.; Lang, Y.; Bleuthmann, H.; Lipp, H-P.; DeArmond, S. J.; Prusiner, S. B.; Aguet, M.; Weissmann, C. Normal development and behaviour of mice lacking the neuronal cell surface PrP protein. Nature 356:577–582; 1992.
9. Caughey, B.; Race, R. E.; Chesebro, B. Detection of prion protein mRNA in normal and scrapie-infected tissues and cell lines. J. Gen. Virol. 69:711–716; 1998.
10. Clough, J.; Whittingham, D. G. Metabolism of [^{14}C] glucose by postimplantation mouse embryos *in vitro*. J. Embryol. Exp. Morphol. 74:133–142; 1983.
11. Collinge, J.; Whittington, M. A.; Sidle, K. C. L.; Smith, C. J.; Palmer, M. S.; Clarke, A. R.; Jefferys, J. G. R. Prion protein is necessary for normal synaptic function. Nature 370:295–297; 1994.
12. Farquhar, C. F.; Somerville, R. A.; Ritchie, L. A. Postmortem immunodiagnosis of scrapie and bovine spongiform encephalopathy. J. Virol. Methods 24:215–221; 1989.
13. Harris, D. A.; Lele, P.; Snider, W. D. Localisation of the mRNA for a chicken prion protein by *in situ* hybridisation. Proc. Natl. Acad. Sci. USA 90:4309–4313; 1993.
14. Hope, J.; Norton, L. J. D.; Farquhar, C. F.; Multhaup, G.; Beyreuther, K.; Kimberlin, R. H. The major polypeptide of scrapie-asociated fibrils (SAF) has the same size, charge distribution and N-terminal protein sequence as predicted for the normal brain protein. EMBO J. 5: 2591–2597; 1986.
15. Hunter, E. S.; Tugman, J. A. Inhibitors of glycolytic metabolism affect neuralation-staged mouse conceptuses *in vitro*. Teratology 52:317–323; 1995.
16. Hunter, N.; Manson, J. C.; Charleson, F. C.; Hope, J. Comparison of expression patterns of PrP messenger-RNA in the developing sheep and mouse. Ann. NY Acad. Sci. 724:353–354; 1994.
17. Jimenez-Huete, A.; Lievens, P. M. J.; Vidal, R.; Piccardo, P.; Ghetti, B.; Tagliavini, F.; Frangione, B.; Prelli, F. Endogenous proteolytic cleavage of normal and disease-associated isoforms of the human prion protein in neural and non-neural tissues. Am. J. Pathol. 153:1561–1572; 1998.
18. Kaufman, M. H. The atlas of mouse development. London: Academic Press Ltd.; 1992.
19. Kimberlin, R. H.; Walker, C. A. Pathogenesis of mouse scrapie: Dynamics of agent replication in spleen, spinal cord and brain after infection by different routes. J. Comp. Pathol. 89:551–562; 1979.
20. Lazarini, F.; Deslys, J-P.; Dormont, D. Regulation of the glial fibrillary acidic protein, β-actin and prion protein mRNAs during brain development in mouse. Mol. Brain Res. 10:343–346; 1991.
21. Lieberburg, L. Developmental expression and regional distribution of the scrapie-associated protein messenger-RNA in the rat central nervous system. Brain Res. 417:363–366; 1987.
22. Mackler, B.; Grace, R.; Duncan, H. M. Studies of mitochondrial development during embryogenesis in the rat. Arch. Biochem. Biophys. 144:603–610; 1971.
23. Manson, J. C.; Clarke, A. R.; Hooper, M. L.; Aitchison, L.; McConnell, I.; Hope, J. 129/Ola mice carrying a null mutation in PrP that abolishes mRNA production are developmentally normal. Mol. Neurobiol. 8: 121–127; 1994.
24. Manson, J. C.; Clarke, A. R.; McBride, P. A.; McConnell, I.; Hope, J. PrP gene dosage determines the timing but not the final intensity or distribution of lesions in scrapie pathology. Neurodegeneration 3:331–340; 1994.
25. Manson, J.; West, J. D.; Thomson, V.; McBride, P.; Kaufman, M. H.; Hope, J. The prion protein gene: A role in mouse embryogenesis? Development 115:117–122; 1992.
26. McKinley, M. P.; Bolton, D. C.; Prusiner, S. B. A protease resistant protein is a structural component of the prion protein. Cell 35:57–62; 1983.
27. McKinley, M. P.; Hay, B.; Lingappa, V. R.; Lieberburg, I.; Prusiner, S. B. Developmental expression of prion protein gene in brain. Dev. Biol. 121:105–110; 1987.
28. Miele, G.; Jeffrey, M.; Turnbull, D.; Manson, J.; Clinton, M. Ablation of cellular prion protein affects mitochondrial numbers and morphology. Biochem. Biophys. Res. Comm. 291:372–377; 2002.
29. Miele, G.; MacRae, L.; McBride, D.; Manson, J.; Clinton, M. Elimination of false positives generated through PCR re-amplification of differential display cDNA. Biotechniques 25:138–144; 1998.
30. Miki, A.; Fujimoto, E.; Ohsaki, T.; Mizoguti, H. Ef-

fects of oxygen concentration on embryonic development in rats—a light and electron microscopic study using whole embryo culture techniques. Anat. Embryol. 178:337–343; 1988.
31. Moser, M.; Colello, R. J.; Pott, U.; Oesch, B. Developmental expression of the prion protein in glial-cells. Neuron 14:509–517; 1995.
32. Moudjou, M.; Frobert, Y.; Grassi, J.; La Bonnardiere, C. Cellular prion protein status in sheep: Tissue-specific biochemical signatures. J. Gen. Virol. 82:2017–2024; 2001.
33. Oesch, B.; Westaway, D.; Walchli, M; McKinley, M. P; Kent, S. B. H.; Aebersold, R.; Barry, R. A.; Tempst, P.; Teplow, D. B.; Hood, L. E.; Prusiner, S. B.; Weissmann, C. A cellular gene encodes scrapie PrP 27-30 protein. Cell 40:735–746; 1985.
34. Pan, K-M.; Baldwin, M.; Nguyen, J.; Gasset, M.; Serban, A.; Groth, D.; Mehlhorn, I.; Huang, Z.; Fletterick, R. J.; Cohen, F.; Prusiner, S. B. Conversion of α-helices into β-sheets features in the formation of the scrapie prion proteins. Proc. Natl. Acad. Sci. USA 90: 10962–10966; 1993.
35. Pauly, P. C.; Harris, D. A. Copper stimulates endocytosis of the prion protein. J. Biol. Chem. 273:33107–33110; 1998.
36. Prusiner, S. B. Novel proteinaceous particles cause scrapie. Science 216:136–144; 1982.
37. Prusiner, S. B. Prions. Proc. Natl. Acad. Sci. USA 95: 13363–13383; 1998.
38. Robakis, N. K.; Sawh, P. R.; Wolfe, G. C.; Rubenstein, R.; Carp, R. I.; Innis, M. A. Isolation of a cDNA clone encoding the leader peptide of prion protein and expression of the homologous gene in various tissues. Proc. Natl. Acad. Sci. USA 83:6377–6381; 1986.
39. Rudd, P. M.; Endo, T.; Colominas, C.; Groth, D.; Wheeler, S. F.; Harvey, D. J.; Wormald, M. R.; Serban, H.; Prusiner, S. B.; Kobata, A.; Dwek, R. A. Glycosylation differences between the normal and pathogenic prion protein isoforms. Proc. Natl. Acad. Sci. USA 96:13044–13049; 1999.
40. Rugh, R. The mouse: Its development and reproduction. New York: Oxford University Press; 1990.
41. Sakaguchi, S.; Katamine, S.; Shigematsu, K.; Nakatani, A.; Moriuchi, R.; Nishida, N.; Kurokawa, K.; Nakaoke, R.; Sato, H.; Jishage, K. Accumulation of proteinase K-resistant prion protein (PrP) is restricted by the expression level of normal PrP in mice inoculated with a mouse-adapted strain of the Creutzfeldt-Jakob disease agent. J. Virol. 69:7586–7592; 1995.
42. Sambrook, J.; Fritsch, E. F.; Maniatis, T. Molecular cloning: A laboratory manual. New York: Cold Spring Harbor Laboratory Press; 1989.
43. Shaked, Y.; Rosenmann, H.; Talmor, G.; Gabizon, R. A C-terminal-truncated PrP isoform is present in mature sperm. J. Biol. Chem. 274:32153–32158; 1999.
44. Stahl, N.; Borchelt, D. R.; Hsiao, K.; Prusiner, S. B. Scrapie prion protein contains a phosphatidylinositol glycolipid. Cell 51:229–240; 1987.
45. Stahl, N.; Borchelt, D. R.; Prusiner, S. B. Differential release of cellular and scrapie prion proteins from cellular membranes by phosphatidylinositol-specific phospholipase C. Biochemistry 29:5405–5412; 1990.
46. Stimson, E.; Hope, J.; Chong, A.; Burliname, A. L. Site-specific characterization of the N-linked glycans of murine prion protein by high-performance liquid chromatography/electrospray mass spectrometry and exoglycosidase digestions. Biochemistry 38:4885–4895; 1999.
47. Stockel, J.; Safar, J.; Wallace, A. C.; Cohen, F. E.; Prusiner, S. B. Prion protein selectively binds copper(II) ions. Biochemistry 37:7185–7193; 1998.
48. Tanji, K.; Saeki, K.; Matsumoto, Y.; Takeda, M.; Hirasawa, K.; Doi, K.; Onodera, T. Analysis of PrP^{C} mRNA by *in situ* hybridisation in brain, placenta, uterus and testis of rats. Intervirology 38:309–315; 1995.
49. Tanimura, T.; Shepard, T. H. Glucose metabolism by rat embryos *in vitro*. Proc. Soc. Exp. Biol. Med. 135: 51–54; 1970.
50. Telford, N. A.; Hogan, A.; Franz, C. R.; Schultz, G. A. Expression of genes for insulin and insulin-like growth factors and receptors in early postimplantation mouse embryos and embryonal carcinoma cells. Mol. Reprod. Dev. 27:81–92; 1990.
51. Tobler, I.; Gaus, S. E.; Deboer, G. T.; Achermann, P.; Fischer, M.; Rulick, T.; Moser, M.; Oesch, B.; McBride, P. A.; Manson, J. C. Altered circadian rhythms and sleep in mice devoid of prion protein. Nature 380: 639–642; 1996.
52. Turrens, J. F. Superoxide production by the mitochondrial respiratory chain. Biosci. Rep. 17:3–8; 1997.
53. Turrens, J. F.; Alexandre, A.; Lehninger, A. L. Ubisemiquinone is the electron donor for superoxide formation by complex III of heart mitochondria. Arch. Biochem. Biophys. 237:408–414; 1985.
54. Wilkinson, D. G. Whole-mount *in situ* hybridisation of vertebrate embryos. In: Wilkinson D. G., ed. *In situ* hybridisation: A practical approach. Oxford: IRL Press; 1992:75–83.